X-ray Absorption Spectroscopic Study of "Costa Type" Organocobalt Coenzyme B12 Models

6 AUTHORS, INCLUDING:

Marco Giorgetti
University of Bologna
85 PUBLICATIONS   1,272 CITATIONS

SEE PROFILE

Mario Berrettoni
University of Bologna
91 PUBLICATIONS   1,769 CITATIONS

SEE PROFILE

Paolo Conti
University of Camerino
21 PUBLICATIONS   178 CITATIONS

SEE PROFILE

Andrea Di Cicco
University of Camerino
205 PUBLICATIONS   3,976 CITATIONS

SEE PROFILE

X-ray Absorption Spectroscopic Study of "Costa Type" Organocobalt Coenzyme B$_{12}$ Models

Marco Giorgetti,[†,‡] Mario Berrettoni,[§] Paolo Conti,[†] Andrea Di Cicco,[§]
Roberto Marassi,[*,†] and Isabella Ascone[‡]

*Dipartimento di Scienze Chimiche, Università di Camerino, via S. Agostino 1,
62032 Camerino (MC), Italy, Dipartimento di Matematica e Fisica, Università di Camerino,
via Madonna delle Carceri, 62032 Camerino (MC), Italy, and LURE Bâtiment 209 D,
Université de Paris-Sud, 91405 Orsay, France*

This paper presents the results of an X-ray absorption spectroscopy (XAS) study of six "Costa type" organocobalt B$_{12}$ model compounds [LCo(DO)(DOH)$_{pn}$R]ClO$_4$, where L = H$_2$O and (DO)(DOH)$_{pn}$ = N^2,$N^{2'}$-propanediylbis(2,3-butanedione 2-imine 3-oxime) and the R groups are different axial alkyl ligands. The dibromo and dichloro complexes [Co(DO)(DOH)$_{pn}$X$_2$] have been studied as well. The structural data obtained from the EXAFS spectra, namely the Co−C bond lengths, have been correlated with the pK_a and Taft σ^* of the alkyl group.

Introduction

The importance of the biochemical role[1,2] of vitamin B$_{12}$ has led, in recent years, to a great effort in the search for organocobalt model compounds with a metal binding as similar as possible to that of the corrin ring. Among the different model compounds (refs 3−5 and references therein) the most studied are the so-called "Costa type" organocobalt complexes,[6] [LCo(DO)(DOH)$_{pn}$R]ClO$_4$
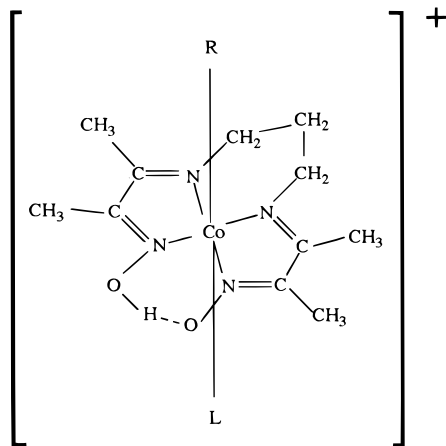
(L = neutral base, (DO)(DOH)$_{pn}$= N^2,$N^{2'}$-propanediylbis(2,3-butanedione 2-imine 3-oxime), and R = alkyl ligand), where the equatorial ligand exhibits the closest

electrochemical behavior to the corrin ring of any B$_{12}$ model. [Note: In order to simplify the notation in the text that follows the molecular formula of the organocobalt complexes will be written as [RCo^{III}L]ClO$_4$, where R = alkyl ligand and L represents the tetradentate (DO)(DOH)$_{pn}$ ligand including one water molecule.]

The physical properties of these compounds have been reviewed.[7−10] Their properties critically depend on the nature of R and hence on the strength of the Co−C bond. The electrochemical reduction mechanism,[11,12] the coordination of the different oxidation states, and the stability of the Co(II) and Co(I) reduced species change with R. Long-lived alkyl derivatives with the metal in low oxidation state have been obtained only in the presence of N-donor heterocyclic ligands[13] or when R is a particularly bulky alkyl group.[11,14] X-ray diffraction data for crystalline "Costa type" model compounds have been published for the methyl,[15,16] isopropyl, and benzyl[17] derivatives and for the dichloro complex.[18]

This paper is the first of a series dealing with XAS (X-ray absorption spectroscopy) studies of the local structure around the cobalt site in "Costa type" compounds with different axial alkyl ligands. This part deals with the study of the solid compounds where the

† Dip. Scienze Chimiche.
‡ Université de Paris-Sud.
§ Dip. Matematica e Fisica.
⊗ Abstract published in *Advance ACS Abstracts,* July 1, 1996.
(1) Halpen, J. *Science* **1985,** *227,* 869.
(2) Brennan, C. L.; Huang, S.; Drummond, J. T.; Matthews, R. G.; Ludwig, M. L. *Science* **1994,** *226,* 1669.
(3) Gerli, A.; Sabat, M.; Marzilli, L. G. *J. Am. Chem. Soc.* **1992,** *114,* 6711.
(4) Marzillli, L. G.; Gerli, A.; Clafat, A. M. *Inorg. Chem.* **1992,** *31,* 4617.
(5) Altink, R.; van Arkel, B.; van der Baan, J. L.; de Bolster, M. W. G.; van Delf, R. J.; Klumpp, G. W.; de Kronig, H.; van der Winkel, Y. *Recl. Trav. Chim.* **1994,** *329,* 1113.
(6) Costa, G.; Mestroni, G.; de Savorgnani, E. *Inorg. Chim. Acta.* **1969,** *3,* 323.

(7) Parker, W. O.; Bresciani Pahor, N.; Zangrando, E.; Randaccio, L.; Marzilli, L. G. *Inorg. Chem.* **1986,** *25,* 1303.
(8) Parker, W. O.; Zangrando, E.; Bresciani Pahor, N.; Randaccio, L.; Marzilli, L. G. *Inorg. Chem.* **1986,** *25,* 3489.
(9) Parker, W. O.; Zangrando, E.; Bresciani Pahor, N.; Marzilli, P. A.; Randaccio, L.; Marzilli, L. G. *Inorg. Chem.* **1988,** *27,* 2170.
(10) Yohannes, P. G.; Bresciani Pahor, N.; Randaccio, L.; Zangrando, E.; Marzilli, L. G. *Inorg. Chem.* **1988,** *27,* 4738.
(11) Seeber, R.; Marassi, R.; Parker, W. O., Jr.; Marzilli, L. G. *Organometallics* **1988,** *6,* 1672.
(12) Seeber, R.; Marassi, R.; Parker, W. O., Jr.; Kelly, G. *Inorg. Chim. Acta* **1990,** *168,* 127 and references therein.
(13) Elliot, C. M.; Hersenhart, E.; Finke, R. G.; Smith, B. L. *J. Am. Chem. Soc.* **1981,** *103,* 5558.
(14) Costa, G.; Puxeddu, A.; Reisenhofer, E. *Experientia Suppl.* **1971,** *18,* 235.
(15) Bruckner, S.; Calligaris, M.; Nardin, G.; Randaccio, L. *Inorg. Chim. Acta* **1969,** *3,* 278.
(16) Parker, W. O., Jr.; Bresciani Pahor, N.; Zangrando, E.; Randaccio, L.; Marzilli, L. G. *Inorg. Chem.* **1985,** *24,* 3908.
(17) Zangrando, E.; Parker, W. O., Jr.; Bresciani Pahor, N.; Thomas, L. B.; Marzilli, L. G.; Randaccio, L. *Gazz. Chim. Ital.* **1987,** *117,* 307.
(18) Nasakkala, M.; Saarinen, H.; Korvenranta, J.; Nasakkala, E. *Acta. Chem. Scand.* **1979,** *A33,* 431.

Table 1. Compounds Studied

compd	ligands (R)	formula
I	isopropyl	$[C_3H_7Co^{III}L]ClO_4$
II	isobutyl	$[C_4H_9Co^{III}L]ClO_4$
III	benzyl	$[C_7H_7Co^{III}L]ClO_4$
IV	methyl	$[CH_3Co^{III}L]ClO_4$
V	methyl acetate	$[C_3H_5O_2Co^{III}L]ClO_4$
VI	2,2,2-trifluoroethyl	$[C_2H_2F_3Co^{III}L]ClO_4$
VII	dichloro	$[Cl_2Co^{III}L]$
VIII	dibromo	$[Br_2Co^{III}L]$

formal oxidation state of cobalt is three. Solutions and XAS spectroelectrochemical studies, where the formal oxidation state of cobalt is changed by electrochemical means, will be the subject of later communications. XAS is a powerful technique to determine the geometrical structure around a selected absorbing atom. Recently it has been demonstrated[19,20] that the EXAFS analysis, performed by taking into account the multiple scattering contributions, gives very accurate structural information on bond lengths and angles. Previous XAS studies of native and reduced vitamin B_{12} have been published by Wirt et al.[21-23]

Experimental Section

The compounds studied, prepared as described elsewhere[10] and characterized by ^{1}H NMR spectroscopy,[9] are listed in Table 1. The samples for XAS measurements were prepared by mixing powdered compounds with cellulose (Merck) (20:80 by weight) and pelletized at 3 tons of pressure.

Experiments were carried out at the D21 experimental station at the DCI storage ring of LURE (Orsay, France) with a positron beam energy of 1.85 Gev and a maximum current of 310 mA. X-ray absorption measurements were performed at Co K-edge using the Si(311) double crystal monochromator. Harmonics were rejected by mirrors with a cut-off at 10 keV. Spectra were recorded in transmission mode. The samples were cooled to a temperature of about 20 K using a liquid-helium cryostat. EXAFS spectra were collected at 2 eV steps and with an integration time of 8 s in the 7600−8600 eV energy range.

Results and Discussion

Figure 1 shows the raw absorption data (a), the EXAFS signal (b), and the Fourier Transform (FT) (c) for $[C_6H_5CH_2Co^{III}L]ClO_4$ that has been chosen to illustrate the procedure followed for data analysis. The FT is dominated by the peak of the first coordination shell at about 1.5 Å. The position of this peak in the FT signal, taking into account the phase shift, corresponds to the average first-shell coordination distance.

Data analysis has been performed by using the package GNXAS.[24,25] The GNXAS method is based on a decomposition of the EXAFS signal into a sum of contributions $\gamma^{(n)}$ associated with the n-body configurations in the environment of the photoabsorber. The two-atom configurations are described by a single mean distance R, while the three-atom configurations are defined by the two shortest distances and by the angle
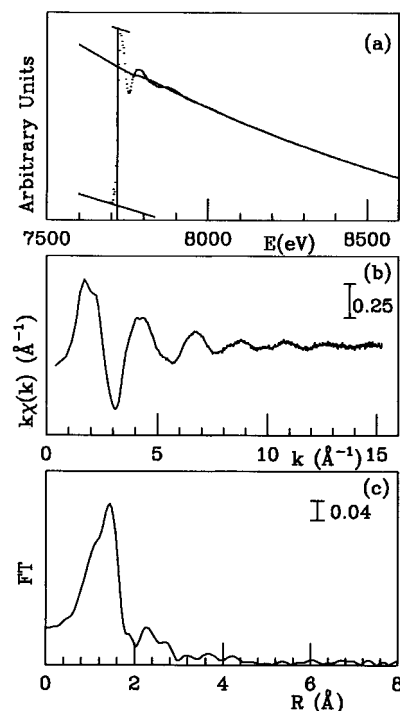
(19) DiCicco, A.; Berrettoni, M. *Phys. Lett. A* **1993**, *176*, 375.
(20) DiCicco, A.; Berrettoni, M.; Stizza, S.; Bonetti, E.; Cocco, G. *Phys. Rev. B* **1994**, *50*, 12386.
(21) Wirt, M. D.; Sagi, I.; Chen, E.; Frisbie, S. M.; Lee, R.; Chance, M. R. *J. Am. Chem. Soc.* **1991**, *113*, 5299.
(22) Sagi, I.; Wirt, M. D.; Chen, E.; Frisbie, S.; Chance, M. R. *J. Am. Chem. Soc.* **1990**, *112*, 8639.
(23) Wirt, M. D.; Sagi, I.; Chance, M. R. *Biophys. J.* **1992**, *63*, 412.
(24) Di Cicco, A. *Physica B* **1995**, *208, 209*, 125.
(25) Filipponi, A.; Di Cicco, A.; Tyson, T. A.; Natoli, R. *Solid State Commun.* **1991**, *78*, 265.

Figure 1. XAS data for compound **III**: (a) Experimental EXAFS row data and splines for atomic background subtraction; (b) k-weighted EXAFS data; (c) FT of the k-weighted EXAFS signal.
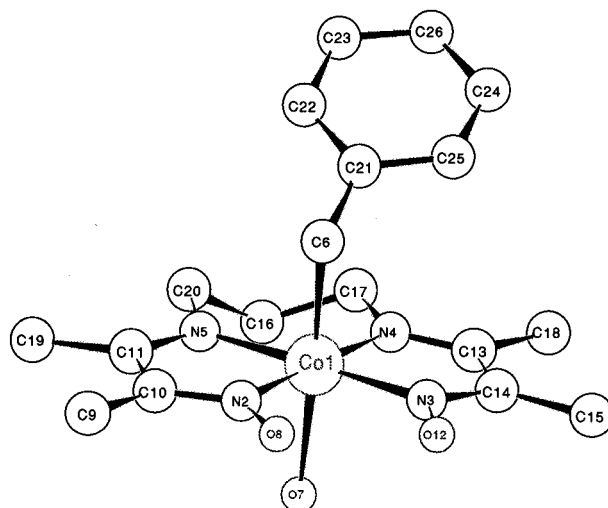

Figure 2. "Ball and stick" structure of compound **III**, showing the atom-numbering system used in the text.

θ in between. The $\gamma^{(2)}$ contains the single and the multiple scattering (MS) contributions associated with the two-body atom configuration. $\gamma^{(n)}$ where $n > 2$, contains all the multiple scattering contributions associated with the n-atom configuration. The total signal obtained by the ab-initio calculations is compared with the experimental spectrum to refine the structural parameters (bond lengths, bond angles, Debye−Waller type factors). The GNXAS program can perform a fit of the experimental raw data (without any filtering procedure) using a standard square residual function that permits statistical analysis of the results. In order to apply the package the most significant MS signals must be determined using a structural model such as the one shown in Figure 2. This has been traced for the benzyl derivative used to test the fitting procedure because its structure has been resolved by X-ray.[17]

With reference to the structure in Figure 2 and taking into account that EXAFS is sensitive to the contributions of atoms up to 4−5 Å from the photoabsorbing atom, the following two-atom contributions have been taken into account: Co_1-N_{2-5}, Co_1-C_6, Co_1-O_7, $Co_1-O_{8,12}$, $Co_1-C_{10,11,13,14}$, $Co_1-C_{17,20,21}$. Each notation indicates either a bond length or the distance between two atoms. Multiple subscripts correspond to the degeneracy of the path. The three-atom configurations of appreciable intensity included into the ab-initio calculation are Co−N−C and Co−N−O.

The fitting procedure was performed directly on the experimental X-ray absorption coefficient with a background contribution that takes into account the opening of two-electron absorption channels.[26−29] An additional edge due to the double-electrons [1s−3p] channel was introduced in the atomic smooth background. In the present case the double excitation energy onset lies at 67 ± 5 eV after the K edge in very good agreement with the $Z + 1$ approximation. Its intensity is $2 \pm 1\%$ of that of the main absorption edge.

The final number of parameters optimized in the fit is 18: 2 parameters, bond length and variance, for the two- and three-atom contributions (16 parameters) plus two nonstructural parameters, E_0 and S_0^2 (many body amplitude reduction factor). The values of S_0^2 for all the studied compounds have been found between 0.92 and 0.94, while the relevant E_0's values are within 4 eV from the edge inflection point. The number of floating parameters is much lower than the number of independent points:[30]

$$N_{ind} = ((2 \; \delta k \; \delta R)/\pi) + 2$$

which gives a rough estimate of the maximum number of parameters that may be fitted with statistical significance. In the definition of N_{ind}, δk is the interval in the k space where the spectrum is defined and δR is the finite interval in the space R used to analyze the spectrum. In our case, $\delta k = 12.7$ and $\delta R = 3.1$ and, hence, $N_{ind} = 27$. Figure 3, panel a, shows the EXAFS signals associated with the selected atomic configurations resulting from the best fit procedure. In Figure 3 panel b the total theoretical signal is compared with the experimental data. The agreement between the experimental and theoretical signals is rather good as may be seen from panel c, where the residual is plotted on an enlarged scale. It is clear from the figure that the intensities of the $Co_1-O_{8,12}$, $Co_1-C_{10,11,13,14}$, $Co_1-C_{17,20,21}$, and Co−N−C, and Co−N−O signals are low when compared with the first-shell paths Co_1-N_{2-5}, Co_1-C_6, and Co_1-O_7. For this reason, the results of the fitting procedure are rather insensitive to the variation of the geometrical parameters associated with the above-mentioned two- and three-body configurations. Therefore, those parameters were allowed to float only within the errors quoted in the X-ray structure[17] of the initial model. In all the other compounds, only the first-shell structural parameters have been refined using, therefore, a very limited number of floating variables.
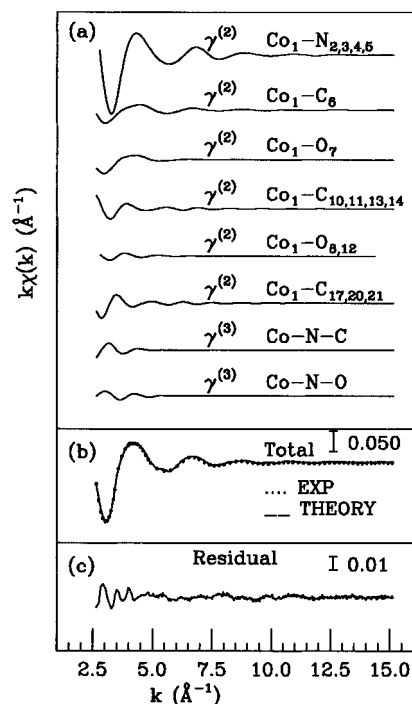
(26) Di Cicco, A.; Stizza, S.; Filipponi, A.; Boscherini, F.; Mobilio, S. *J. Phys. B* **1992**, *25*, 2309.

(27) Burattini, E.; D'Angelo, P.; Di Cicco, A.; Filipponi, A.; Pavel, N. V. *J. Phys. Chem.* **1993**, *97*, 5486.

(28) Li, G.; Bridges, F.; Brown, G. S. *Phys. Rev. Lett.* **1992**, *68*, 1609.

(29) Frenkel, A. I.; Stern, E. A.; Quian, M.; Newville, M. *Phys. Rev. B* **1993**, *48*, 12449.

(30) Stern, E. A. *Phys. Rev B* **1993**, *48*, 9825.

Figure 3. Comparison of the theoretical and experimental signals of the k-weighted EXAFS data for compound **III**: (a) individual contributions of the different $\gamma^{(n)}$ signals; (b) total theoretical (−−) and experimental (···) k-weighted EXAFS signals; (c) residual as given by the difference between the theoretical and experimental k-weighted EXAFS signal.
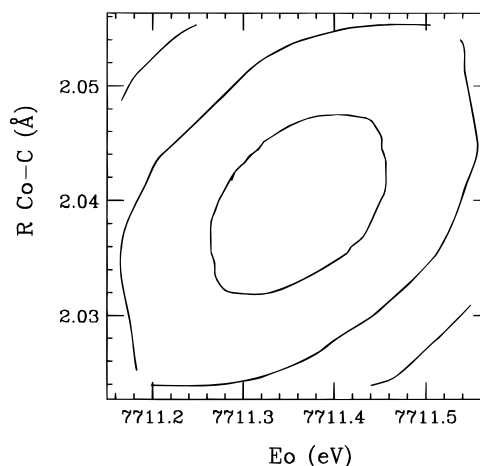

Figure 4. Two-dimensional section of the parameter space referring to R and E_0 for compound **III**. The inner elliptical contour corresponds to the 95% confidence interval.

In order to establish the error associated with the fitted main structural parameters, an additional statistical analysis[31,32] was performed. The contour plot of the highly correlated E_0 and Co−C variables is shown in Figure 4 (only for compound **III**). As may be seen, at 95% confidence level (inner ellipse), the statistical error in bond length is lower than 0.01 Å, in line with the precision normally quoted for a complex crystalline system.[33]

The relevant structural information obtained from the fit is summarized in Table 2 together with the existing X-ray diffraction data. The results obtained for the

(31) Filipponi, A.; Di Cicco, A. *Phys. Rev B* **1995**, *52*, 15135.

(32) Filipponi, A. *J. Phys.: Condens. Matter* **1995**, *7*, 9343.

(33) Di Cicco, A.; Sperandini, F. *Phys. C* **1996**, *258*, 349.

Table 2. Relevant Bond Length Fitting Results, EXAFS Bond Variances, and X-ray Diffraction Data for the Compounds I–VIII

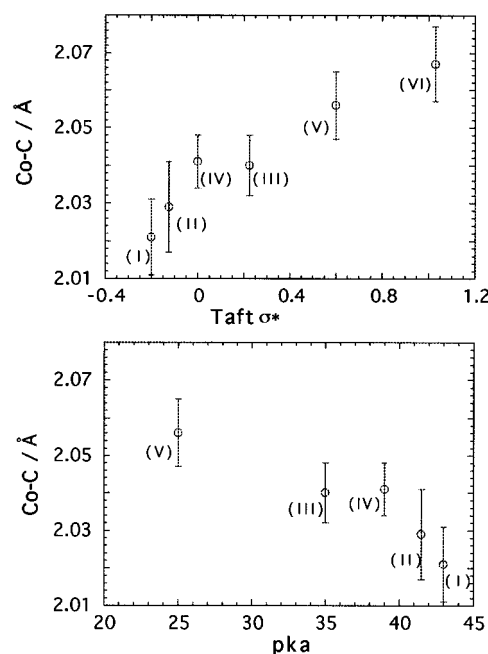| compd	method	$Co-N_{2-5}$/Å (degeneracy = 4)	$Co-N_{2-5}$ var[a]	$Co-C_6$/Å (degeneracy = 1)	$Co-C_6$ var[a]	$Co-O_7$/Å (degeneracy = 1)	$Co-O_7$ var[a]
I	EXAFS	1.887	0.003	2.021(10)[b]	0.005	2.160	0.012
	cryst[c]	1.898[d] [1.877–1.920]		2.055		2.138	
II	EXAFS	1.874	0.005	2.029(12)[b]	0.006	2.159	0.011
III	EXAFS	1.883	0.005	2.040(8)[b]	0.007	2.102	0.015
	cryst[c]	1.904[d] [1.886–1.928]		2.052		2.099	
IV	EXAFS	1.888	0.003	2.041(7)[b]	0.006	2.127	0.015
	cryst[e]	1.90[d] [1.86–1.94]		1.99		2.14	
V	EXAFS	1.906	0.003	2.056(9)[b]	0.005	2.206	0.015
VI	EXAFS	1.896	0.003	2.067(10)[b]	0.007	2.219	0.015
				$Co-X_{6,7}$/Å (degeneracy = 2)	$Co-X_{6,7}$ var[a]		
VII	EXAFS	1.893	0.003	2.225	0.005		
	cryst[f]	1.913[d] [1.90–1.930]		2.250[d] [2.247–2.254]			
VIII	EXAFS	1.886	0.003	2.378	0.005		

[a] Bond variance (var) values resulting from thermal and structural disorder are reported in Å². [b] Statistical error as from two-dimensional contour plots (see text for details). [c] Values from ref 17. [d] These values are average distances; ranges are in brackets. [e] Values from ref 15. [f] Values from ref 18.
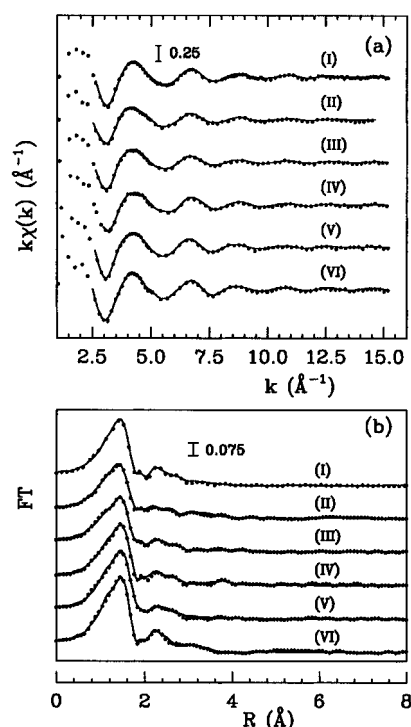
Figure 5. Comparison of theoretical (- - -) and experimental (···) k-weighted EXAFS data (panel a) and relative FT (panel b) for compounds **I–VI**.

Figure 6. Co–C bond lengths with error bars vs pK_a and Taft σ^* for compounds **I–VI**.

alkyl and halide derivatives are discussed separately in the following sections.

Alkyl Substituents. Figure 5 shows the comparison of the best fit with the experimental data (panel a) and the corresponding FT (panel b) for all the alkyl-substituted compounds. As can be seen, the agreement between the experimental and theoretical curves is rather good in all cases. The four Co–N bond lengths (Table 2) are rather close for all compounds. This means that the out-of-plane groups do not have a large influence on the backbone of the tetradentate ring. Optimization of the fitting procedure by considering the four Co–N distances separately or different combinations of two of them results in bond lengths within the estimated bond length variance.

Because of the rigidity of the in-plane atom network and of the relatively high variance of the Co_1-O_7 bond length (Table 2), indicating a weakly bound transaxial

group with a weak associated EXAFS signal, any variation of the first peak position in the FT spectrum must be associated mainly with the influence of the alkyl group. The lengths of the Co–C bonds vary from 2.021 to 2.067 Å and may be associated with the pK_a of hydrocarbon acid R–H or with the Taft σ^*,[34] an inductive (polar) substituent parameter: i.e. the weaker the acid (or the lower the inductive effect), the shorter the bond. This is apparent from Figure 6, where the Co–C bond lengths, together with the associated estimated errors, are plotted vs the pK_a and Taft σ^* of the alkyl group. Compound VI, for which, to the best of our knowledge, the pK_a data are not available, is not plotted. However, from simple considerations of inductive effects, it should be located in the upper left corner of the plot.

As a final consideration, one may observe that the bulkiness of the substituent does not seem to be correlated with the Co–C bond length as appears to be the

(34) Taft, R. W. *J. Am. Chem. Soc.* **1952**, *74*, 3120; *J. Am. Chem. Soc.* **1953**, *75*, 4231.
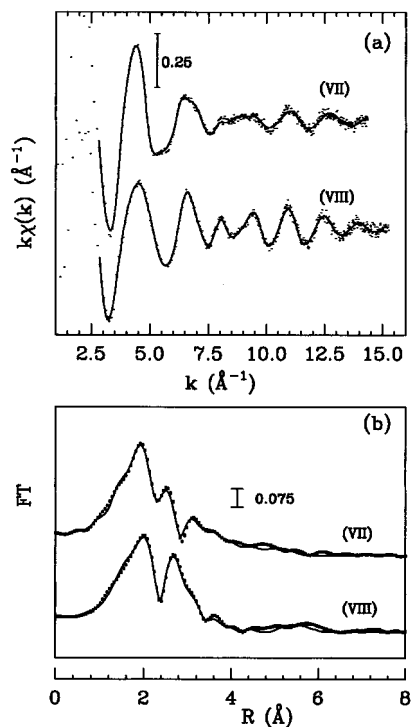
Figure 7. Comparison of theoretical (- - -) and experimental (···) *k*-weighted EXAFS data (panel a) and relative FT (panel b) for compounds **VII** and **VIII**.

case in other series of compounds[35] where the bond length increases with increasing steric hindrance of the alkyl group. No correlation has been found between the Taft E_s,[34] a parameter related to the steric properties of the substituent, and the bond lengths. This leads to the conclusion that the bond length does not depend on the bulkiness of the alkyl groups. However, XANES spectra presently under investigation[36] indicate that the steric hindrance may move the cobalt out of the equatorial plane.

Halide Ligands. Figure 7 shows the theoretical and the experimental EXAFS and related FT for compounds **VII** and **VIII**, where the axial groups are chloride and bromide, respectively. The total theoretical signal is practically identical to the experimental. Because of the higher scattering power of the halide atoms and the greater intensity of multiple scattering contributions, EXAFS oscillations are seen in the overall range of the energy and in the related FT spectrum up to 5 Å from the absorbing atom. The two Co−X (Cl or Br) bonds cause splitting of the transformed signal at distances corresponding to the first shell.[18]

Figure 8 shows the theoretical contributions to the total EXAFS signal, as obtained from the best fit, of the $\gamma^{(n)}$ distributions for compound VIII. The frequency that dominates the total spectrum is $\gamma^{(2)}$ of the Co−Br bonds. The relative Co−X bond lengths are 2.225 and 2.378 Å, respectively, for chloride and bromide reflecting the relative dimensions of the two atoms. As may be seen from Table 2, the Co−N$_{2-5}$ distances are almost the
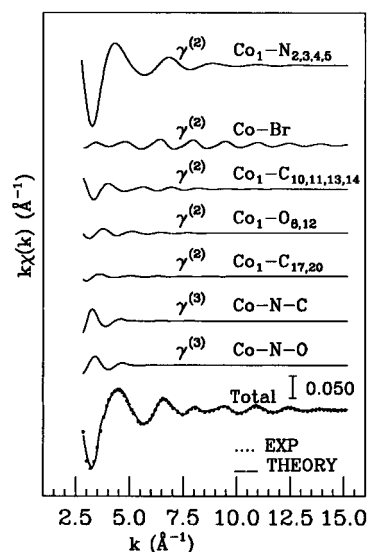
(35) Tavagnacco, C.; Balducci, G.; Costa, G.; Taschler, K.; von Philipsborn, W. *Helv. Chim. Acta.* **1990**, *73*, 1469.
(36) Giorgetti, M.; Berrettoni, M.; Marassi, R.; Ascone, I. To be published.

Figure 8. Comparison of the theoretical and experimental signals of the *k*-weighted EXAFS data for compound **VIII**: (a) individual contributions of the different $\gamma^{(n)}$ signals; (b) total theoretical (--) and experimental (···) *k*-weighted EXAFS signals.

same for both compounds and the agreement between the EXAFS and X-ray diffraction data is rather good. In the case of the dichloro compound, in order to obtain a good agreement between the theoretical and experimental data, it is necessary to include in the calculation the three-body signal related to the collinear Cl−Co−Cl configuration (angle of 180°). In the case of the dibromo compound, because of the longer bond, the EXAFS spectrum is less sensitive to the three-body signal as demonstrate by the direct calculation performed using bond angles in the range 120−180°. On the contrary, in the case of dichloro compound, the variation of the mean angle of few a degrees is found to determine a substantial increase of the residual.

Conclusions

EXAFS data of "Costa type" analogs of coenzyme B₁₂ have been accurately studied using an "ab-initio" multiple scattering data-analysis procedure (GNXAS). The short-range structural parameters related to the metal site obtained by EXAFS have been found in agreement with the available X-ray diffraction data. New information on the (metal−ligand) bond length distribution has been extracted in several Costa type compounds for which X-ray diffraction data are not available. The EXAFS analysis of several Costa type analogs of coenzyme B₁₂ has permitted the study of the Co−C bond length dependence on the nature of the alkyl group. In particular the bond length, and hence the strength of the bond, appears to depend on the pK_a and Taft σ^* constant of the alkyl group. No dependence of the bond length on the steric hindrance of the alkyl group has been observed. In the case of the dihalide complexes, the bond lengths appear to depend on the dimensions of the halide atoms.